Rapid and complete hitless defragmentation method using a coherent RX LO with fast wavelength tracking in elastic optical networks

Rapid and complete hitless defragmentation method using a coherent RX LO with fast wavelength tracking in elastic optical networks

Roberto Proietti,* Chuan Qin, Binbin Guan, Yawei Yin, Ryan P. Scott, Runxiang Yu, and S. J. B. Yoo

Department of Electrical and Computer Engineering, University of California, Davis, One Shields Ave., Davis, California 95616, USA
**rproietti@ucdavis.edu*

Abstract: This paper demonstrates a rapid and full hitless defragmentation method in elastic optical networks exploiting a new technique for fast wavelength tracking in coherent receivers. This technique can be applied to a single-carrier connection or each of the subcarriers forming a super-channel. A proof-of-concept demonstration shows hitless defragmentation of a 10 Gb/s QPSK single-carrier connection from 1547.75 nm to 1550.1 nm in less than 1 μs. This was obtained using a small (0.625 kB) link-layer transmitter buffer without the need for any additional transponder. We also demonstrated that the proposed defragmentation technique is capable of hopping over an existing connection, *i.e.* 10 Gb/s OOK at 1548.5 nm, without causing any degradation of its real-time Bit Error Rate (BER) value. The proposed scheme gives advantages in terms of overall network blocking probability reduction up to a factor of 40.

OCIS codes: (060.4256) Networks, network optimization; (060.4265) Networks, wavelength routing; (060.1660) Coherent communications.

References and links

1. M. Jinno, H. Takara, B. Kozicki, Y. Tsukishima, Y. Sone, and S. Matsuoka, "Spectrum-efficient and scalable elastic optical path network: architecture, benefits, and enabling Technologies,"," IEEE Commun. Mag. **47**(11), 66–73 (2009).
2. Y. Yin, K. Wen, D. J. Geisler, R. Liu, and S. J. Yoo, "Dynamic on-demand defragmentation in flexible bandwidth elastic optical networks," Opt. Express **20**(2), 1798–1804 (2012).
3. A. N. Patel, P. N. Ji, J. P. Jue, and T. Wang, "Defragmentation of transparent flexible optical WDM (FWDM) networks," (Optical Society of America, 2011), p. OTuI8.
4. T. Takagi, H. Hasegawa, K.-i. Sato, Y. Sone, A. Hirano, and M. Jinno, "Disruption minimized spectrum defragmentation in elastic optical path networks that adopt distance adaptive modulation," (Optical Society of America, 2011), p. Mo.2.K.3.
5. F. Cugini, M. Secondini, N. Sambo, G. Bottari, G. Bruno, P. Iovanna, and P. Castoldi, "Push-pull technique for defragmentation in flexible optical networks," in *Optical Fiber Conference* (2012), p. JTh2A.40.
6. K. Sone, X. Wang, S. Oda, G. Nakagawa, Y. Aoki, I. Kim, P. Palacharla, T. Hoshida, M. Sekiya, and J. C. Rasmussen, "First demonstration of hitless spectrum defragmentation using real-time coherent receivers in flexible grid optical networks," in *European Conference on Optical Communication* (2012), p. Th.3.D.1.
7. G. Bosco, V. Curri, A. Carena, P. Poggiolini, and F. Forghieri, "On the performance of Nyquist-WDM terabit superchannels based on PM-BPSK, PM-QPSK, PM-8QAM or PM-16QAM subcarriers,"," J. Lightwave Technol. **29**(1), 53–61 (2011).
8. L. A. Coldren, G. A. Fish, Y. Akulova, J. S. Barton, L. Johansson, and C. W. Coldren, "Tunable semiconductor lasers: A tutorial,"," J. Lightwave Technol. **22**(1), 193–202 (2004).
9. R. Maher, D. Millar, S. Savory, and B. Thomsen, "Widely tunable burst mode digital coherent receiver with fast reconfiguration time for 112Gb/s DP-QPSK WDM networks," J. Lightwave Technol. **99**, 1 (2012).
10. B. C. Thomsen, R. Maher, D. S. Millar, and S. J. Savory, "Burst mode receiver for 112 Gb/s DP-QPSK with parallel DSP," Opt. Express **19**(26), B770–B776 (2011).

#176651 - $15.00 USD Received 21 Sep 2012; revised 6 Nov 2012; accepted 6 Nov 2012; published 15 Nov 2012

11. S. J. B. Yoo, H. J. Lee, Z. Pan, J. Cao, Y. Zhang, K. Okamoto, and S. Kamei, "Rapidly switching all-optical packet routing system with optical-label swapping incorporating tunable wavelength conversion and a uniform-loss cyclic frequency AWGR," Photonics Technol. Letters **14**, 1211–1213 (2002).

1. Introduction

Elastic optical networking [1] is a promising approach for achieving efficient spectrum utilization in a network by allocating just-enough bandwidth to each user's demands. In contrast to traditional WDM networks, the spectrum is divided into arbitrary or smaller frequency units (*e.g.* 12.5 or 25 GHz, also known as optical subcarriers). This enables various connections (flexpaths) to use an arbitrary number of subcarriers depending on their bandwidth demands. However, this added flexibility also raises new challenges such as spectral fragmentation [2]. Since the fragments are neither contiguous in the frequency domain nor aligned along a path, they become stranded bandwidths that can hardly be utilized by new connection requests. Spectral defragmentation, which aims at re-optimizing the spectrum utilization, typically involves rerouting or re-assignment of the spectrum location of existing connections [3].

Ref [4]. presents a disruption-minimized make-before-break (MbB) technique exploiting the rerouting solution to do defragmentation. Ref [5, 6] proposes wavelength sweeping hitless defragmentation methods that leverage the automatic frequency control (AFC) capabilities of coherent receivers. However, the MbB method requires an additional transmitter to provide an extra connection while the wavelength sweeping methods cannot achieve complete defragmentation without disrupting other existing connections.

Here we propose and experimentally demonstrate a new technique to achieve a full defragmentation operation with very short latency (< 1 μs) which causes no service disruption (hitless) by using a small amount of link layer buffer (*e.g.* 100 Gb/s subcarrier would need less than 12.5 kB buffer during defragmentation). Under the assumption of using Nyquist WDM [7] transponders, the fast-tuning receiver (RX) local oscillator (LO) can rapidly auto-track a change in the transmitter (TX) wavelength when defragmentation operation takes place. This automatic tracking functionality removes the need for end-to-end handshaking between TX and RX. Further, the combination of the fast tuning speed of superstructure grating distributed Bragg reñector (SSG-DBR) lasers [8], the blanking of the optical emission from the SSG-DBR laser during the tuning, and the buffering of the bits during the tuning, allows the proposed technique to move the spectrum of the connection without interrupting services of any existing connections including those of itself. Compared with the MbB technique [4], the proposed defragmentation method does not require additional transponders. Compared with other techniques based on continuously and slowly sweeping TX/RX lasers [5, 6], the proposed method achieves complete defragmentation even if active connections exist between the current and the target spectral location for the connection to be defragmented, resulting in faster defragmentation time and reduced blocking probability. Table 1 summarizes the advantages and disadvantages of the above discussed defragmentation approaches.

Table 1. Comparison of Defragmentation Techniques

	Additional TXs/RXs.	Defrag. Time	Interfering with other connections?
Sweeping	No	s	yes
MbB	Yes	ms	no
This paper	No	μs	no

#176651 - $15.00 USD Received 21 Sep 2012; revised 6 Nov 2012; accepted 6 Nov 2012; published 15 Nov 2012

The remainder of the paper is organized as follows: Section II shows a network scenario with undergoing defragmentation. The analysis shows that our technique can guarantee faster defragmentation time and lower blocking probability compared to what can be achieved with wavelength sweeping techniques [5, 6]. Section III discusses the hitless defragmentation testbed. We introduce the coherent RX with fast wavelength tracking, which is at the core of our defragmentation technique, and show a proof-of-concept experimental demonstration of the defragmentation technique using a three-node network testbed. Section IV concludes by highlighting the main results presented in this manuscript and by summarizing future directions.

2. Network performance of different defragmentation techniques

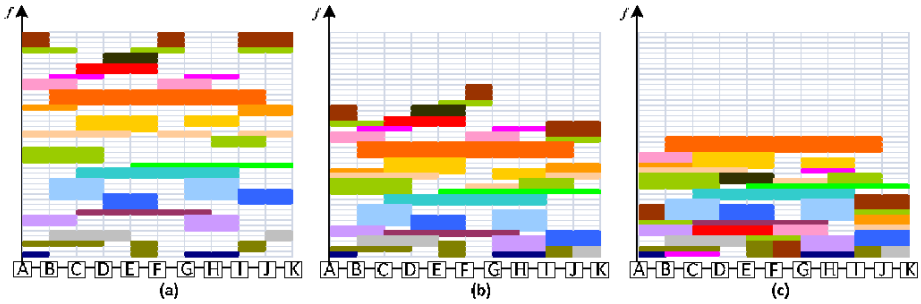

Fig. 1. Spectrum diagram (a) before defragmentation, (b) after sweeping defragmentation, and (c) after complete defragmentation using the proposed method.

Among all the proposed defragmentation schemes, the rerouting based make-before-break [4] technique requires additional transponder resources to set up the rerouted connection (or connection on the same route but with different wavelength) before tearing down the original one. Although the techniques in [5, 6] do not require additional transponder resources, the use of a spectrum sweep method by exploiting the AFC capabilities of coherent receivers results in incomplete defragmentation due to the fact that the sweeping spectrum cannot cross over the other fragments in the network. Figure 1 shows an example. When the spectral resources in a ten-link linear network are fragmented as shown in Fig. 1(a), the wavelength sweeping technique can only tune the signals to sweep over an empty spectral range to fill the "gap" without interfering with other live traffics. In other words, the only possible way of retuning is to let the signals occupying the slots above the empty slots "fall down" to fill in the blank. Then the defragmentation process continues to sweep the neighboring connections to fill the gap left behind by the previous operation. In the end, the defragmentation operation will simply stop after doing its best without interrupting other connections. The best achievable defragmentation result using wavelength sweeping in this example is shown in Fig. 1(b). Another disadvantage of this method is that the entire network must go through this defragmentation in proper sequence, tuning the spectrum one by one, resulting in sequential accumulation of the tuning time by the individual transmitters. On the contrary, the proposed fast tuning and tracking defragmentation technique can quickly "jump over" any amount of spectral range in any sequence and in parallel, regardless of the existence of a live connection within the spectral range. In the end, the best achievable defragmentation result is shown in Fig. 1(c), which is considered to be a fully defragmented spectrum map resulting in the most compact occupation of the spectrum. Moreover, it is notable that the overall time needed to achieve the best defragmentation results differs significantly between the two compared methods. The sweeping technique tunes the connections one by one to sweep over each one's spectrum range in sequence to achieve the best result. In other words, there is a dependency map [6] which determines the proper sequence of tuning the signals. The time required for completing the defragmentation operation is estimated as (# of vacated slots + # of signal

#176651 - $15.00 USD Received 21 Sep 2012; revised 6 Nov 2012; accepted 6 Nov 2012; published 15 Nov 2012

layers −1) × λ sweep time per slot [6]. The # of signal layers is related to the dependency map, while a reasonable assumption of λ sweep time is (100ms/2.5 GHz) × (12.5GHz/Slot) = 500ms/Slot [6]. On the other hand, the proposed method can fast tune the connections with very short latency (< 1 μs). The latency for each defragmentation operation is given by the time it takes for the TX and LO lasers to switch to the new wavelength and reach a stable condition (frequency offset below ± baud-rate/8 for the carrier phase recovery being able to work). The higher the baud-rate, the lower is the latency. This latency is also quite independent from the distance between the initial and target wavelength, while in [5, 6], the latency is proportional to this distance.

Network simulations have been carried out to compare the performance of the proposed method versus the wavelength sweeping technique. Dynamic connection arrival and departure events are simulated on a 14-node NSFNET network. For simplicity, the flexible-grid WSS switches are assumed at each node with synchronized operations to cooperate with the defragmentation tasks. Each spectral slot is assumed to be 12.5 GHz and each fiber link has 400 slots. In the simulation, 6,000 ~10,000 connection requests with randomly chosen source and destinations arrive according to a Poisson process. The holding time of each connection follows an exponential distribution with average value of 5 time units. The connection bandwidth is randomly distributed from 4 spectral slots (50 GHz) to 12 slots (150 GHz).

Defragmentation operations are triggered when a group of n connections (n = 30 in this case) depart the network. For comparison, simulations were run under same conditions except for the wavelength sweeping technique, which has to follow the tuning sequence to avoid interference when there is a gap in the spectrogram. We assume the sweep speed is 500 ms/Slot as suggested in [6], while in the proposed technique the defragmentation latency is always below 1 μs regardless the target spectral positions.

Figure 2(a) shows that defragmentation can significantly or marginally reduce the bandwidth blocking probability (BBP) depending on the defragmentation method used. However, there is a factor of 40 improvement (at load of 300 Erlangs) using the proposed technique compared with the sweeping technique. In terms of average time per defragmentation operation, Fig. 2(b) shows that the proposed technique outperforms the sweeping technique by a few orders of magnitude. The sweeping technique (incompletely) conducts defragmentation in 1.2 seconds at load of 300 Erlangs, while the proposed method completes it in 7 μs. Note that the defragmentation time decreases with traffic load for both techniques because the defragmentation algorithm completes in less time when there is less room to tune the connections.

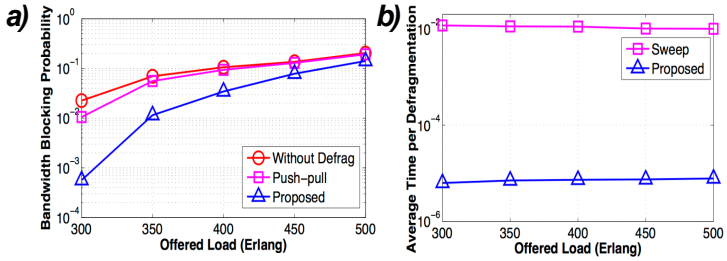

Fig. 2. Comparison of wavelength sweeping technique and proposed technique in terms of (a) blocking probability vs. offered load, and (b) average network defragmentation time per signal departure vs. offered load.

3. Hitless defragmentation experiment

3.1 Network scenario

Figure 3(a) depicts a simple 3-node network scenario for proof-of-concept demonstration of the proposed defragmentation technique. Each node is equipped with elastic optical

#176651 - $15.00 USD Received 21 Sep 2012; revised 6 Nov 2012; accepted 6 Nov 2012; published 15 Nov 2012

transponders (EOTN) and reconfigurable optical add and drop multiplexers (ROADMs), which can be wavelength selective and/or colorless.

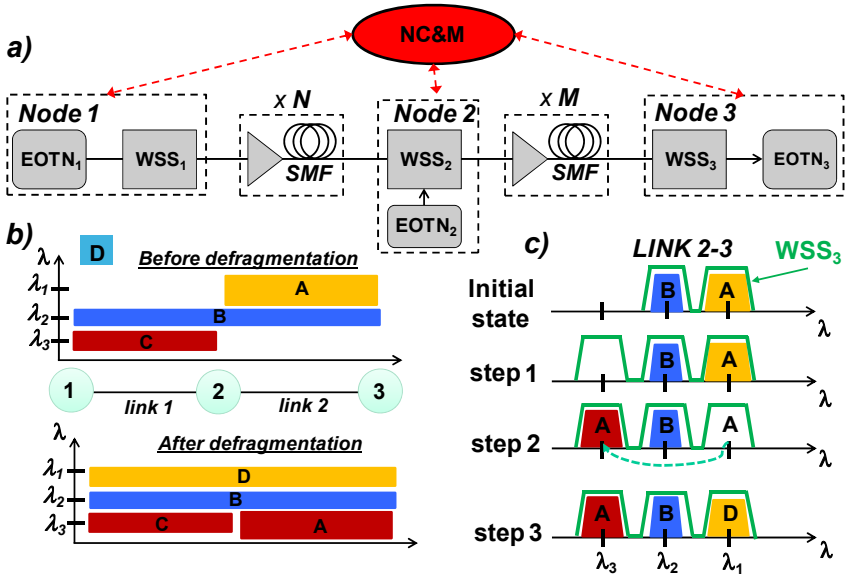

Fig. 3. (a) 3-node network scenario: EOTN - elastic optical transponder; WSS: wavelength selective switch; NC&M: network control and management. (b) spectrum allocation before (top) and after (bottom) defragmentation. (c). Defragmentation steps with WSS reconfiguration to accept the new spectrum position for connection A.

Figure 3(b) shows the spectrum allocation of the different connections on the different links before and after the defragmentation operation. Let us assume that Node 1 wishes to establish a new connection **D** to Node 3. On link 1 a certain number of frequency slots are available around the center frequency corresponding to λ_1. However, the same spectrum is not available on link 2. An efficient usage of the spectrum resources would require then to move connection **A** (orange) to λ_3 (dark red). In this way spectrum resources can be made available on link 2 to establish the new connection **D**. The question is: how to achieve this operation without having to disrupt any existing connection for a long time or requiring additional transponders? Next section addresses this question.

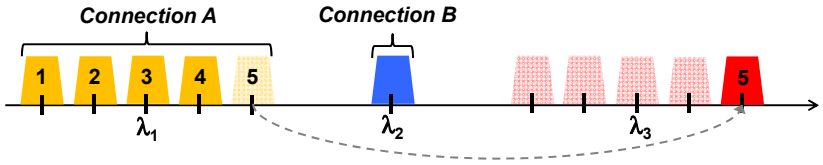

Fig. 4. Example of connection A occupying 5 frequency slots centered at lambda1 before (left) and after defragmentation. Each subcarrier composing the superchannel is generated using a fast TLD and it is received with a coherent receiver using a fast TLD as LO.

3.2 Coherent RX with fast wavelength tracking – architecture and working principle

Figure 4 shows an example in which connection **A** occupies 5 frequency slots centered at λ_1 before defragmentation (left). After the defragmentation connection **A** is then centered at λ_3 (right). Each subcarrier composing the superchannel is generated using a fast TLD and it is received with a coherent receiver using a fast TLD as LO (see Fig. 5). Figure 5 shows how to address the question above. A fast-tuning tunable laser diode (TLD) acts as LO in the proposed coherent RX. The incoming signal (*e.g.* connection **A** from WSS3 shown in Fig.

#176651 - $15.00 USD Received 21 Sep 2012; revised 6 Nov 2012; accepted 6 Nov 2012; published 15 Nov 2012

4(b) and Fig. 5) is tapped and sent to the input of an athermal AWG with a certain frequency grid (*e.g.* 12.5 or 25 GHz). The *N* AWG outputs then connect to an array of low-speed photo-detectors (PD array) to monitor the optical power at the different spectrum locations in order to determine whether there is a change in the wavelength position of the incoming connection. If the subcarriers wavelengths of connection **A** change, the PD array outputs will generate a transition from 0 V to a certain value. A field-programmable gate array (FPGA) can use this transition to understand the new wavelength positions and fast tuning the local oscillators (LO) in the transponders to track the new wavelength values of the incoming connection. Let us assume that the network control and management (NC&M) decide to defragment moving connection **A** to λ_3. First it will send control signals to reconfigure the various network elements on link 2-3, *i.e.* wavelength selective switches, like shown in Fig. 3(c). Then, the NC&M will send a control message to EOTN2 to start the defragmentation, which can be done one subcarrier at a time or all the subcarriers together. Let us focuses on one single subcarrier.

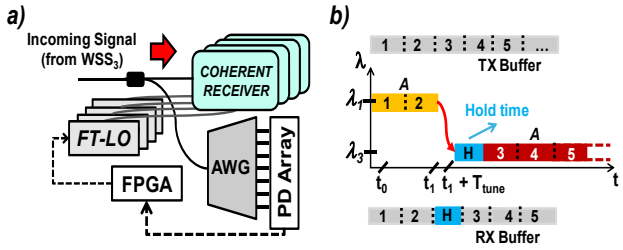

Fig. 5. (a) Bank of coherent receivers with fast-tuning local oscillators (FT-LOs) with wavelength tracking based on athermal AWG and a PD Array. (b): Time/Frequency domain representation of defragmentation operation for connection A.

As shown in Fig. 5, at time instant t_1, after transmission of frame 2 is completed, the EOTN in Node 2 quickly tunes one subcarrier wavelength from λ_1 to λ_3, holding the transmission for the time necessary for the FT-LO to track the new TX wavelength and the coherent receiver to lock. Then it restarts the transmission of the next frame in the buffer. At the application layer, such buffering can be properly accommodated to avoid an interruption in services. Keeping this hold time as short as possible is our target in order to use a small amount of link-layer buffer and guarantee very small latency and no hit at the service layer. At time instant "$t_1 + T_p + T_{tune}$" (T_p is the propagation time), PD3 (3rd PD in the PD array) will sense a transition which will quickly trigger the tuning of the LO to λ_3. From then on, the digital coherent receiver can start the synchronization procedure, which can be as fast as few hundreds of ns (T_{LOCK}), as demonstrated in [9]. The hold time, T_{HOLD}, can be calculated as follows:

$$T_{HOLD} = T_{tune\_TX} + T_{LOOP} + T_{tune\_LO} + T_{LOCK} \quad (1)$$

T_{tune_TX} and T_{tune_LO} are the tuning time for the TX and the LO respectively and are well below 100 ns [8]. T_{LOOP} is the time needed to recognize a transition at the PD output and to send the control signal to the fast TLD LO. This time is short and depends on the PD bandwidth and the FPGA clock speed. Assuming 500 MHz for both PD and FPGA, the process can complete in 10 ns (a few FPGA clock cycles). Then, based on Eq. (1), the hold time could be < 500 ns. If we assume a subcarrier with 100 Gb/s traffic (25 GBd QPSK with polarization multiplexing), this would correspond to a link-layer buffer of ~6.1 kB. Note that when the TX laser tunes, it must avoid interference with other connections such as connection **B** at λ_2 in Fig. 3(b). The method described in this paper achieves this by using fast tuning and blanking function in SSG-DBR lasers [8].

#176651 - $15.00 USD Received 21 Sep 2012; revised 6 Nov 2012; accepted 6 Nov 2012; published 15 Nov 2012

Note that, in theory, it would be possible to control the defragmentation operation from the NC&M and remove the need of the AWG-based feedback loop shown in Fig. 5. In practice, this would add a lot of complexity in the network control plane. In fact, in order to minimize the defragmentation latency while requiring minimum amount of buffering and no data loss, it is necessary to minimize the amount of time the TX and LO lasers have a frequency offset bigger than ± baud-rate/8 [9]. If the defragmentation is entirely controlled by the NC&M, the NC&M would need to send the defragmentation control messages for switching the TX and LO lasers synchronously, calculating exactly the propagation time between NC&M and TX, between NC&M and RX, and between the TX and the RX. For these reasons the wavelength tracking function of Fig. 5 is essential.

In case of a 12.5 GHz grid, a 400 port AWG and 400 photodetectors (PDs) would be necessary, which is possible but complex. A practical approach, that still has all the advantages summarized in Table1, can be to use the proposed technique on a coarser grid, *e.g.* 50 GHz. In this way, 100 PDs and 100 port AWG would be sufficient. Our technique could be then used to quickly move the connection as close as possible to the target wavelength, while the techniques in [5, 6] could be used for fine adjustment of the connection on a finer grid (12.5 or 25 GHz).

3.3 Experimental results of hitless defragmentation in elastic optical network testbed

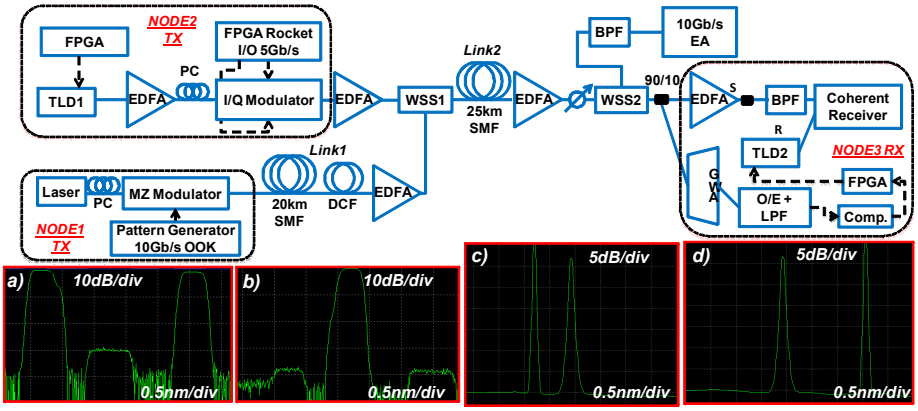

Fig. 6. Hitless defragmentation network testbed. TLD: tunable laser diode; FPGA: field programmable gate array; WSS: wavelength selective switch; LPF: low pass filter; Comp: comparator; EDFA: erbium doped fiber amplifier. BPF: band pass filter. Inset (a) and (b): filtering profile of WSS1 input ports 1 and 2. Insets (c) and (d): spectrum allocation before and after defragmentation.

Figure 6 shows the experimental testbed that recreates the scenario depicted in Fig. 3. The demonstration is given here for a single-carrier connection, but it can be extended to a superchannel scenario (multiple subcarriers) as explained above. Two fast SSG-DBR TLDs (TLD1 and TLD2) are used as TX laser and LO (laser linewidth is 2 MHz and output power is 0 dBm) to generate and receive connection **A**, which is a 10Gb/s QPSK signal in this experiment. An FPGA provides defragmentation signal for switching TLD1. The two Rocket I/O of the Virtex5 FPGA generate two 5 Gb/s RF binary signals that drive an I/Q modulator. Each Rocket I/O pulled out data stored in two buffers on the FPGA. The data correspond to PRBS sequences 2^7 - 1 long. The resulting signal is 10Gb/s QPSK, which is then amplified and launched into a 25 km single-mode fiber (SMF) link through a wavelength selective switch (WSS1). At the RX side, the signal passes through a second WSS (WSS2), an attenuator, an EDFA, and a band-pass-filter. WSSs profile are shown in the insets of Fig. 6. Then the signal enters in a coherent receiver with offline digital signal processing, which includes clock recovery, equalization and carrier phase recovery. 10% of the signal power at WSS2 output feeds a feedback loop with an AWG (100 GHz spacing in this example), an O/E

#176651 - $15.00 USD Received 21 Sep 2012; revised 6 Nov 2012; accepted 6 Nov 2012; published 15 Nov 2012

converter, a low pass filter (250 MHz) and a threshold comparator. The FPGA monitors the comparator output and sends a control signal to the TLD LO to rapidly track the TX wavelength, as explained in the previous section. The clock speed of FPGA is 312.5 MHz, which generates the 5 GBd line rate using the high speed Rocket IO. The FPGA clock speed affects the speed of controlling the tunable lasers. Specifically, when the PD-array detects the change of the wavelength in the incoming signal and reports to the FPGA LO controller, the FPGA can only respond and tune the LO after 1 clock cycle (3.2 ns).

The second input of WSS1 is fed with a 10Gb/s OOK connection at $\lambda_{2,}$, which represents connection **B** in the scenario of Fig. 3. Connection **B** is dropped at output 2 of WSS2 and monitored with a 10 Gb/s error analyzer (EA). A switch on the FPGA board activates the defragmentation operation by switching TLD1 wavelength from λ_1 to $\lambda_{3.}$ The EA monitors the BER of the connection B lying in between λ_1 and λ_3 during the defragmentation operation. In this experiment, the values of λ_1, λ_2, and λ_3 are 1547.75 nm, 1548,5 nm and 1550.1 nm respectively.

During the switching of TLD1 wavelength, Rocket IOs hold the data transmission from their buffers for 512 ns in order to allow enough time for the coherent RX to lock at the new wavelength λ_3. Once locked, Rocket IOs start to transmit the data again. In this way no data is lost, and at the application layer, no interruption would be noticed, which is a necessary requirement to guarantee hitless operation.

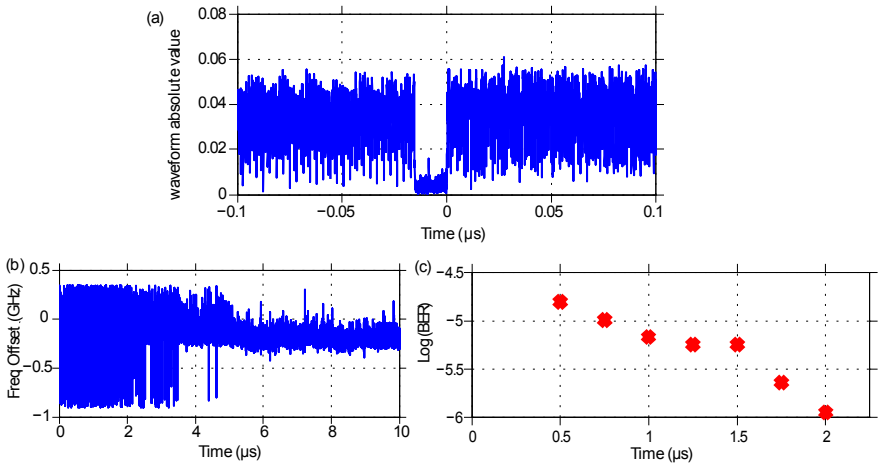

Fig. 7. (a) trace showing the time when defragmentation happens. (b) Frequency offset between TX and LO lasers after they switched to lambda3 VS time; (c) BER VS time instant from which DSP processing and BER counting start.

Figure 7(a) shows a real-time scope trace showing the time when defragmentation happens. The real time scope used for sampling the signal was running at 25 GSample/s. The ~20ns gap in Fig. 7(a) is the time required by the two TLDs (TX and LO) to reach λ_3 with an offset much smaller than the photo-detectors bandwidth (3-dB bandwidth of 40 GHz). The meaningful data starts only after ~(512 −20) ns from the end of the 20ns gap. The reason for choosing T_{HOLD} = 500 ns can be understood from Fig. 7(b) and Fig. 7(c). In order for the carrier phase recovery to work, the frequency offset needs to be within ± baudrate/8. After that, any slow variation can be tracked. Figure 7(b) shows the frequency offset between TX and LO lasers after they reach λ_3 (before DSP carrier frequency/phase estimation). Then, - 0.4 GHz is the frequency difference between the TX and LO frequency after both lasers stabilize. Figure 7(c) shows the BER as function of the time instant from which DSP processing and BER counting start, (after the TLDs reach λ_3). At 0.5 μs, right after the useful data start, BER is well below 10^{-3} even though there are still occasionally some large phase glitches that DSP

#176651 - $15.00 USD Received 21 Sep 2012; revised 6 Nov 2012; accepted 6 Nov 2012; published 15 Nov 2012

cannot recover. As we increase the time instant from which DSP and BER counting starts, the BER performance in Fig. 7(c) becomes better because we basically discard more symbols that carrier phase recovery could not retrieve (because of the frequency offset is bigger than ± baudrate/8). However, at 2 μs the lasers are more stable, and the BER reaches below 10^{-6}, which is the lower bound of meaningful BER value. In fact, for each BER point in Fig. 7(c), we used three acquisition of 180 μs, each one corresponding to 4.5 million samples, given 25 GSample/s. Then, the total number of symbols was 900,000 for each acquisition, for a total of 2,700,000 symbols and 5,400,000 bits.

The offline DSP included standard digital signal processing functions like clock recovery, constant modulus algorithm (CMA) equalizer, and Viterbi-Viterbi algorithm for carrier frequency and phase estimation. We did not include any fiber chromatic dispersion compensation, since the maximum accumulated chromatic dispersion value in this experiment was 17 ps/nm*km × 25km × 0.04nm = 17 ps.

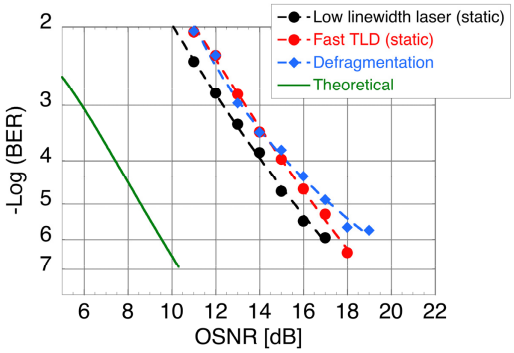

Fig. 8. The BER performance of the elastic optical network. "black dots": BER curve obtained with 100KHz linewidth laser; "red dots": static measurement at λ_3 with 2MHz lasers (fast TLDs); "blue diamonds": BER at λ_3 during defragmentation operation.

Figure 8 shows BER measurements as function of OSNR during defragmentation of connection **A** from λ_1 to λ_3 (in this measurement we started BER counting at 2 μs from the end of the 20 ns gap). We also compared against a laser with 100 kHz linewidth. The penalty is small, indicating that DSP with differential decoding can sustain fast switching burst-mode operation with both TX and LO lasers switching very fast. Note that in our experiment the baud-rate was limited by the FPGA rocket I/O bandwidth. At higher baud-rates, like in [9, 10], the time window in which the frequency offset is bigger than ± baudrate/8 will decrease, making the defragmentation operation even faster.

As mentioned above, an EA monitors in real-time the BER of the connection **B** at λ_2 during the defragmentation operation. Figure 9(a) shows the accumulated BER over different time windows of one minute, and Fig. 9(b) shows the corresponding accumulated errors.

The first measurement shows the BER and accumulated errors of connection **B** when no fragmentation of connection **A** is performed. The results, as expected, show 0 accumulated errors over one minute, which corresponds to a BER ≤ 10^{-11}. The second measurement shows the case when defragmentation operation is performed using the proposed technique. For this measurement we replaced the WSS with a 3 dB coupler to emulate a colorless ROADM. In fact, for this particular example with the WSS, the λ_2 wavelength would be blocked by the WSS itself (see WSS profile in Fig. 6 - insets (a) and (b)). During the one minute time windows, we performed several defragmentation operation from λ_1 to λ_3 and back to λ_1. No errors were recorded. This proves that our technique allows very fast defragmentation without interfering with existing connections. In this experiment we found out that blanking function was not even necessary. In fact, even without TLD blanking, no errors were observed. This can be explained with the fact that during the switching operation from λ_1 to λ_3, no significant

#176651 - $15.00 USD Received 21 Sep 2012; revised 6 Nov 2012; accepted 6 Nov 2012; published 15 Nov 2012

amount of optical power is generated at λ_2. Note that even in the worst case where a significant amount of power at λ_2 is generated, because the switching is very fast (nanoseconds time scale), the amount of time that the signal under defragmentation will take to go across the signal at λ_2 would be in the order of hundreds of picoseconds [11], which leads to a minimal number of bit errors that FEC can correct. However, we understand that, in a general case, blanking function should be used to avoid any possible burst-error problem, especially in the case of high baud-rate per subcarrier.

Finally, a third measurement shows what would happen to connection **B** at λ_2 if we would use the wavelength sweeping techniques. For this measurement, we replaced the fast TLD1 with a wavelength-sweeping external cavity laser sweeping from λ_1 to λ_3 at a speed of 0.5 nm/s.

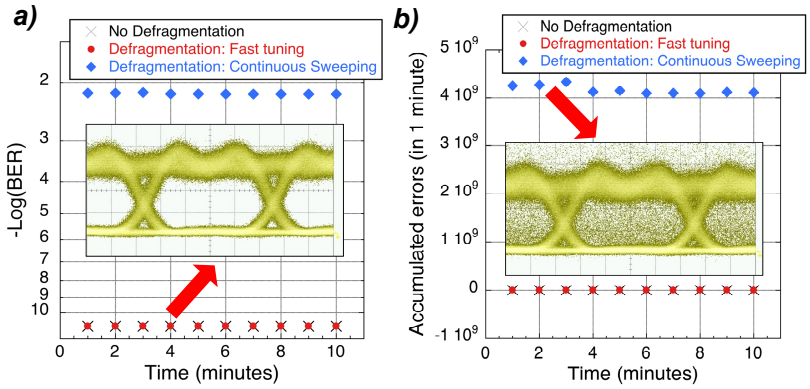

Fig. 9. (a) Real-time BER monitor of connection B at lambda2 and (b) accumulated errors on connection B under different defragmentation scenario. BER and errors are calculated over one minute. "x": no defragmentation operation is performed; "red dots": fast defragmentation with the proposed technique both in case of wavelength selective or colorless ROADM; "blue diamonds": defragmentation based on wavelength sweeping.

The sweep takes about 7 seconds and it starts at the 20th second in each of the one-minute time windows. As we can see the result is catastrophic and the BER goes from 10^{-11} to ~10^{-2} (inset in Fig. 9(b) shows the eye diagram acquired over 1 minute).

4. Conclusions

We proposed and demonstrated a hitless defragmentation method that leads to complete defragmentation of the spectral map in an elastic optical network without relying on sequential tuning of wavelengths. The method utilizes a transmitter with a fast tunable laser and a burst-mode coherent receiver with fast wavelength tracking at the node. By additional blanking and buffering capability, the defragmentation can hop across existing live connections without interrupting each other's services at the application layer. We experimentally demonstrate a hitless defragmentation scheme in the elastic optical network testbed. The fast auto-tracking technique involves an athermal AWG with a detector array sensing a change in the TX wavelength, without the need for end-to-end bi-directional coordination between transmitters and receivers. The experiment conducted here for a single 10 Gb/s QPSK channel achieved defragmentation in less than 1 μs, leading to the requirement for ~0.625 kB memory, and can scale to 1 Tb/s for 62.5 kB memory without significantly increasing the defragmentation time since the tuning of individual wavelengths of multiple transmitters can take place in parallel. In this case, the RX will need to receive specific information from the NC&M in order to differentiate multiple wavelength changes simultaneously. This method can also be used in a modular operation to defragment a Nyquist-WDM superchannel by moving one subcarrier at a time, and can be used in Pol-

#176651 - $15.00 USD Received 21 Sep 2012; revised 6 Nov 2012; accepted 6 Nov 2012; published 15 Nov 2012

Muxed Elastic Optical Networks when polarization modulated or polarization multiplexed transmitters and receivers are used.

Acknowledgments

We acknowledge Nistica for the loan of the WSSs. We would like to acknowledge also Dr. Nicolas Fontaine and Dr. Benn Thomsen for useful discussions on digital signal processing (DSP), and Mr. Mingyang Zhang and Prof. Zuqing Zhu for their help on the networking simulations. This work was supported in part by CISCO URP and Ericsson POPCORN project.

#176651 - $15.00 USD Received 21 Sep 2012; revised 6 Nov 2012; accepted 6 Nov 2012; published 15 Nov 2012